Fast Physics-based Electromigration Analysis for Multi-Branch Interconnect Trees

Xiaoyi Wang*,Yan Yan*,Jian He*,Sheldon X.-D. Tan†,Chase Cook†,Shengqi Yang*
*Beijing Advanced Innovation Center for Future Internet Technology,
Beijing Engineering Research Center for IoT Software and Systems,
Beijing University of Technology, Beijing, China, 100124
†Department of Electrical and Computer Engineering, University of California, Riverside, CA 92521

***Abstract*—Electromigration (EM) becomes one of the most challenging reliability issues for current and future ICs in 10nm technology and below. In this paper, we propose a new analsys method for the EM hydrostatic stress evolution for multi-branch interconnect trees, which is the foundation of the EM reliability assessment for large scale on-chip interconnect networks, such as power grid networks. The proposed method, which is based on eigenfunctions technique, could efficiently calculate the hydrostatic stress evolution for multi-branch interconnect trees stressed with different current densities and non-uniformly distributed thermal effects. The new method can also accommodate the pre-existing residual stresses coming from thermal or other stress sources. The proposed method solves the partial differential equations of EM stress more efficiently since it does not require any discretization either spatially or temporall, which is in contrast to numerical methods such as finite difference method and finite element method. The accuracy of the proposed transient analysis approach is validated against the analytical solution and commercial tools. The efficiency of the proposed method is demonstrated and compared to finite difference method. The proposed method is 10X∼100X times faster than finite difference method and scales better for larger interconnect trees.**

I. Introduction

As technology scaling down to nanometers, the electromigration (EM) becomes a major issue of the chip reliability because of the increasing current density and decreasing size of the interconnects. Therefore, electromigration verification becomes indispensable for chip sign-off.

Traditionally, the statistical Black's equation [1] and Blech limit [2] are employed to predict the EM-induced mean time to failure (MTTF). These EM modeling predicts the MTTF and the immortality for individual branches characterized by known current densities and temperatures. However, these methods are criticized for inaccuracy due to their empirical nature and lack of consideration of residual stress [3]–[5].

Modern interconnect networks consist of interconnect trees representing continuously connected, highly conductive metal wires within one layer of metalization, terminated by diffusion barriers. Recent studies show that the stress evolution in each individual branch of a multi-branch interconnect trees are not independent as EM-induced migrations take place in the whole interconnect tree [6]. In order to consider these effects, some physics-based EM analysis methods for the through silicon via (TSV) and power grid networks have been proposed [3], [6]–[8]. The well accepted model is proposed by Korhonen [9], which is based on the diffusion-like partial differential equations (PDEs) describing the kinetics of hydrostatic stress evolution.

For all those methods based on Korhonen's model, solution to the PDEs of hydrostatic stress is undoubtly the corner stone. However, the requirements of accuracy and efficiency to the solution are conflicting due to the large size of on-chip interconnect networks. As a consequence, the existing methods compromise either on accuracy or efficiency. Finite element analysis (FEA) based method [7] can only solve small structures such as one TSV because of the expensive computational cost. To facilitate the EM analysis of large multi-branch interconnect trees , a compact physics-based EM model was proposed by [6], [8]. These methods mainly focus on the steady-state solution of hydrostatic stress instead of transient hydrostatic stress. Thus these methods cannot provide the accurate time evolution of the hydrostatic stress, which ultimately determines the failures (such as nucleation and void growth) for multi-branch interconnect wires. To mitigate this problem, the finite difference method (FDM) is proposed by [3], [10] to solve the Korhonen's equations. As a general numerical method, the FDM can provide numerical solution of transient hydrostatic stress for general interconnect tree. In addition, the FDM can also accommodate the non-uniform residual stress as well as the non-uniform transient thermal and current effects.

In contrast to the numerical solutions such as FEA and FDM, analytical solutions were also proposed for specific interconnect trees. The first analytical solution was given in the original work of Korhonen [9], describing the hydrostatic stress evolution on a single wire. Although this solution provides insights to the electromigration, it only works for a single wire, the simplest interconnect structure. Recently an analytical modeling was proposed to provide exact expressions describing the hydrostatic stress evolution in several typical interconnect trees, namely the straight-line 3-terminal wires, the T-shaped 4-terminal wires and the cross-shaped 5-terminal wires [11]. However, this method also only works for a few specific wire structures, not for general multi-branch interconnect trees. In order to extend the analytical approach

This work is funded by National Natural Science Foundation of China (NSFC) grants under No. 61602016. This work is supported in part by National Natural Science Foundation (NSF) grant under No. CCF-1527324.

978-1-5386-3093-8/17/$31.00 ©2017 IEEE

to analyze the transient hydrostatic stress evolution for large scale power grid networks, [12] proposed a method utilizing integral transform technique to solve one-dimentional Korhonen's equations for multi-segment wires for a stratight wire, which is a common routing structure of power grid networks. However, this method still can not solve for general tree structure of 2-dimentional interconnect trees. Moreover, these methods lack the ability to accommodate the non-uniformly distributed thermal effects.

Despite the limited interconnect structure they can solve, the analytical solutions have advantages over numerical approaches, especially in efficiency. In this paper, we develop a new method that generalize these analytical solutions to accurate transient analysis of hydrostatic stress for multi-branch interconnect trees. Moreover, the proposed method could also accommodate non-uniform thermal and current effects as well as arbitrary residual stress distribution. As a result, the proposed method can solve the same problems as the numerical methods do, but with the advantages of analytical solutions, as following : 1. the proposed method solves the Korhonen's equations more efficiently since it does not require any discretization, which will reduce the number of unknown variables significantly; 2. it avoids integrating the transient stress over time with small time steps to get the accurate solution. In contrast, it can compute the stress for a specific time directly. 3. Although some parameters are decided numerically, it provides analytical solutions to facilitate more efficient EM analysis techniques, such as searching for the void nucleation time by Newton's method [6], which is effective only if analytical solutions are provided. It's worth to mention that the solution we provide in this work becomes exactly the same as the analytical solutions of single wire [9] or one-dimensional multi-segment interconnect wires [12]. As a fundamental method, the proposed approach can work together with any other acceleration techniques for EM analysis, such as the filtering and predicting techniques proposed in [3].

The paper is organized as following: In section II, the physics-based EM models are reviewed. A novel method is then proposed in section III and IV for accurate transient analysis of hydrostatic stress evolution in void nucleation phase and void growth phase, respectively. The accuracy and efficiency of the proposed method are demonstrated by the experimental results in section V. Finally, we give the conclusion.

II. Review of Physics-based EM Models

EM is a physical phenomenon of the migration of metal atoms along a direction of applied electrical field. The momentum exchange between atoms and the conducting electrons results in metal depletion at the cathode and a corresponding metal accumulation at the anode ends of the metal wire. Since the thin layers of refractive metals form diffusion barriers for Cu atoms preventing them from diffusion into inter-layer (ILD) and inter-metal dielectrics (IMD), as shown by Figure 1, the EM occurs primarily on the interconnect tree, which is a continuously connected, highly conductive metal with one layer of

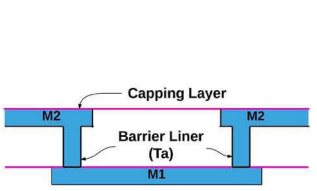

Fig. 1. Layers of Cu Interconnects

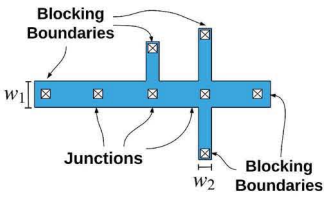

Fig. 2. Interconnect Tree Structure

metallization, terminated by diffusion barriers, as illustrated by Figure 2. As a general interconnect tree, the wires on tree could have different widths and different diffusivity caused by non-uniform thermal distribution. When metal wire is embedded into a rigid confinement, the wire volume changes induced by the atom depletion and accumulation due to migration create tension at the cathode end and compression at the anode end of the wire. The lasting electrical load increases these stresses, as well as the stress gradient along the metal wire. The stress generated inside the embedded metal wire is the prime cause of the void and hillock formation at the opposite ends of the wire. The void nucleation time could be obtained when stress reaches the critical value σ_{crit} and extracted kinetics of the void volume evolution governs the evolution of wire resistance. Degradation of the electrical resistance of interconnect segment due to the void growth can be derived from the solution of kinetics equation describing the time evolution of stress in the interconnect segments [9], [13]–[15].

For a branch of the interconnect tree, the hydrostatic stress evolution $\sigma(x,t)$ could be described as the diffusion-like equation (1), which was proposed by by Korhonen [9] to model the void nucleation and kinetics of void size evolution and further developed by other researchers [13], [14].

$$\frac{\partial \sigma(x,t)}{\partial t} = \frac{\partial}{\partial x}\left[\kappa\left(\frac{\partial \sigma(x,t)}{\partial x} + \mathcal{G}\right)\right] \tag{1}$$

where $\kappa = \frac{D_a B \Omega}{k_B T}$ is the diffusivity of stress, $\mathcal{G} = \frac{E q^*}{\Omega}$ is the EM driving force and D_a is effective atomic diffusion coefficient, defined as (2).

$$D_a = D_0 \exp\left(-\frac{E_a}{k_B T}\right) \tag{2}$$

Here, D_0 is the pre-exponential factor, E_a is the activation energy, B is the effective bulk elasticity modulus, Ω is the atomic lattice volume, k_B is the Boltzmann's constant, T is temperature, E is the electric field, q^* is the effective charge, x is the coordinate along the wire, and t is time. As we can see from above equations, the diffusivity is affected by temperature. Therefore non-uniform distributed temperature results in different diffusivity on each branches.

From Ohm's law, the electric field E could be replaced by the product of resistivity ρ and current density $\jmath$, i.e. $E = \rho\jmath$. The effective charge $q^* = |Z^*|e$ is a known quantity, where e is the elementary charge and $Z = |Z^*|$ is the effective

charge number. As a result, the EM driving force $\mathcal{G}$ could be calculated by equation (3) as a function of current density.

$$\mathcal{G} = \frac{eZ}{\Omega}\rho j \tag{3}$$

On a interconnect tree, atoms diffuse across branch boundaries at junction nodes. As a result, the hydrostatic stress on branches interact with each other, which is confirmed by the fact that diffusion equations of each branches are coupled by boundary conditions on branch ends. For junction nodes on the tree, the boundary conditions (4) represent the facts that the hydrostatic stress should be continuous and the atom flux should be conserved to 0.

$$\begin{aligned} &\sigma_{ij_1}(x = x_i, t) = \sigma_{ij_2}(x = x_i, t) \\ &\sum_i w_{ij} J_{a,ij}(x_i, t) = \sum_i w_{ij}\kappa_{ij}\left(\left.\frac{\partial \sigma_{ij}}{\partial x}\right|_{x=x_i} + \mathcal{G}_{ij}\right) = 0 \end{aligned} \tag{4}$$

where ij represents the branches connected to junction node i, w_{ij} is the cross-section area of branch ij, κ_{ij} is the diffusivity of branch ij, $\sigma_{ij}(x,t)$ is stress distribution on branch ij and $J_{a,ij}(x,t)$ is the atom flux on branch ij.

For nodes at blocking boundaries of the interconnect tree, the atom diffusion is blocked because the metal lines are confined. Therefore, the atom flux at the block boundary is 0, reflected by the boundary condition (5).

$$J_a(x_\ell, t) = \kappa_{\ell j}\left(\left.\frac{\partial \sigma}{\partial x}\right|_{x=x_\ell} + \mathcal{G}_{\ell j}\right) = 0 \tag{5}$$

where ℓ is the node at blocking boundaries.

Under the effect of EM-induced driving force, the hydrostatic stress will build up as tensile stress (i.e. positive stress) or compressive stress (i.e. negative stress). As long as the tensile stress exceeds the critical stress σ_{crit}, the void nucleates. After the void nucleation, the wire comes to the void growth phase, in which the void would enlarge in size as a result of the atom depletion caused by current density. In void growth phase, the void nucleation also causes significant change to the hydrostatic stress [16].As described by extended Korhonen model in [16], the tensile stress at the void surface quickly falls to zero at the void surface but remains its original value a very short distance $\delta = 1nm$ in the void growth phase. Here, the δ is the thickness of the void interface. As a consequence, the boundary condition at void nucleation is described as equation (6).

$$\left.\frac{\partial \sigma(x,t)}{\partial x}\right|_{x=x_\ell} = \frac{\sigma(x_\ell, t)}{\delta} \tag{6}$$

where ℓ is the node at void nucleation.

From the transient analysis, we can see the tensile stress on the void nucleation will be effectively released, which usually leads to the tension release all over the interconnect tree. Besides the change of hydrostatic stress, the wire resistance starts to increase over the time in the void growth phase.

From kinetics of EM-induced void described above, it's clear that the accurate solution to the PDEs (1) is crucial for EM reliability assessment. In the simple case of a single-segment wire, the transient stress could be solved analytically by the technique of separation of variables. The analytical solution could be used to decide the void nucleation time by examining when the hydrostatic stress exceeds the critical stress σ_{crit}. However, in the case of interconnect tree, atoms migrating across branches of tree will eliminate the stress buildup at the unblocked branch ends. In other words, the stress will be effectively distributed all over the interconnect tree according to the current density. So it is important to figure out the hydrostatic stress regarding the interconnect as a whole.

In this paper, we managed to generalize the analytical solution from the special cases such as [11], [12] to the complex case of multi-branch trees, with non-uniform wire sizing, non-uniform diffusivity caused by non-uniform thermal distribution, transient current effects and arbitrary residual stress distribution. Although some parameters are decided numerically, the proposed method provides analytical solutions for hydrostatic stress evolution. The main advantage of this method compared to the numerical approaches such as FDM is the efficiency of computing high accuracy solutions, which will facilitate the realistic EM analysis for the large scale on-chip interconnect networks.

III. Transient Analysis of HydroStatic Stress Evolution in Void Nucleation Phase

The hydrostatic stress evolution on a interconnect tree could be described by a group of coupled PDEs, which is a typical initial-boundary value problem (IBVP). The proposed method first transforms this IBVP to homogeneous problem and utilize the "separation of variables" technique to solve it. It then computes the eigenvalues and eigenfunctions numerically. Next, the coeffcients of eigenfunctions are determined by initial conditions. Finally the transient hydrostatic stress is calculated as a linear combination of eigenfunctions.

A. Steady-State Hydrostatic Stress Distribution and Transformation to Homogeneous Transient Problem

To solve the coupled Korhonen's equations, the governing equation (1) as well as the coupled boundary conditions (5) and (4) should be transformed to homogeneous ones to leverage the use of "separation of variables" technique.

The Korhonen's equations (1) and boundary conditions (5) (4) could be transformed to homogeneous ones by subtracting the transient stress distribution $\sigma(x,t)$ by the steady state stress distribution $\sigma(x,\infty)$. The transformed hydrostatic stress $\hat{\sigma}(x,t)$ is then defined by equation (7).

$$\hat{\sigma}(x,t) = \sigma(x,\infty) - \sigma(x,t) \tag{7}$$

To facilitate this transformation, the steady state hydrostatic stress distribution $\sigma(x,\infty)$ has to be figured out first. The steady state stress problem has already been solved in previous works [17], [18]. We hereby shortly review the steady state stress analysis for convenience. For any branch ij on interconnect tree, the stress distribution comes to steady state when

it stops changing with time, i.e. $\frac{\partial \sigma_{ij}(x,\infty)}{\partial t} = 0$. Substituting this to Korhonen's equation (1), the atom flux is found to be constant in steady state and this constant has to be zero according to boundary conditions (5). This fact is shown by equation (8).

$$J_{a,ij}(x,\infty) = \kappa_{ij}\left(\frac{\partial \sigma_{ij}(x,\infty)}{\partial x} + \mathcal{G}_{ij}\right) = const = 0 \quad (8)$$

From equation (8), it is clear that the steady state stress is linearly distributed on branch ij and satisfies equation (9). In addition, the steady stress is subject to atom conservation equation (10). As a result, the steady state stress $\sigma(x,\infty)$ could be solved explicitly from equation (9) and equation (10).

$$\sigma_{ij}(x_j,\infty) - \sigma_{ij}(x_i,\infty) = l_{ij}\mathcal{G}_{ij} \quad (9)$$

$$\sum_{ij} \frac{\sigma_{ij}(x_j,\infty) + \sigma_{ij}(x_i,\infty)}{2} \cdot l_{ij} \cdot w_{ij} = 0 \quad (10)$$

Using transformation equation (7) and the zero atom flux equation (8) for steady state, it could be proven that the Korhonen's equation is transformed to homogeneous IBVP, which is described by governing equations (11) and boundary conditions (12), (13). For the lack of space, the proof is skipped here.

$$\frac{\partial \hat{\sigma}_{ij}(x,t)}{\partial t} = \kappa_{ij}\frac{\partial^2 \hat{\sigma}_{ij}(x,t)}{\partial x^2} \quad (11)$$

$$\hat{\sigma}_{ij_1}(x = x_i, t) = \hat{\sigma}_{ij_2}(x = x_i, t)$$
$$\sum_i w_{ij} \cdot \kappa_{ij}\frac{\partial \hat{\sigma}_{ij}(x,t)}{\partial x}\bigg|_{x=x_i} \cdot \mathrm{n}_i = 0 \quad (12)$$

$$\kappa_{j\ell}\frac{\partial \hat{\sigma}_{j\ell}(x,t)}{\partial x}\bigg|_{x=x_\ell} = 0 \quad (13)$$

where n_i is the "normal direction" of boundary i on branch ij, which is $+1$ for right end and -1 for left end of branch.

Meanwhile, the initial conditions are transformed as equation (14).

$$\hat{\sigma}(x,0) = \sigma(x,\infty) - \sigma(x,0) = \sigma(x,\infty) - \sigma_T \quad (14)$$

B. Solving the Transient Problem by Separation of Variables

Since being transformed to homogeneous equations, the initial-boundary value problem (11) (12) (13) (14) is ready for separation of variables. The solution $\hat{\sigma}_{ij}(x,t)$ is assumed to be separated into two parts : $\psi_{ij}(x)$ and $\Gamma(t)$, as shown by equation (15).

$$\hat{\sigma}_{ij}(x,t) = \psi_{ij}(x) \cdot \Gamma(t) \quad (15)$$

Substituting equation (15) to equation (11), the partial differential equations could be separated into two ordinary differential equations (ODEs) as following:

$$\frac{\kappa_{ij}}{\psi_{ij}(x)}\frac{\partial^2 \psi_{ij}(x)}{\partial x^2} = \frac{1}{\Gamma(t)}\frac{\partial \Gamma(t)}{\partial t} = -\lambda^2 \quad (16)$$

where λ is the eigenvalue. As a matter of fact, the eigenvalues consist of an infinite series $0 \leqslant \lambda_1 \leqslant \lambda_2 \leqslant \cdots \leqslant \lambda_m \leqslant \cdots$.

For each eigenvalue, there are two equations to solve : one transient equation (17) with respect to temporal function $\Gamma(t)$ and another equation (18) with respect to spatial distribution $\psi_{ij}(x)$.

$$\frac{d\Gamma(t)}{dt} + \lambda_m^2 \Gamma(t) = 0 \quad (17)$$

$$\frac{\partial^2 \psi_{ij,m}(x)}{\partial x^2} + \frac{\lambda_m^2}{\kappa_{ij}}\psi_{ij,m}(x) = 0 \quad (18)$$

The general solutions to equation (17) and equation (18) are well known as equation (19) and (20) , respectively.

$$\Gamma(t) = C_m \cdot e^{-\lambda_m^2 t} \quad (19)$$

$$\psi_{ij,m}(x) = A_{ij,m}\sin\left(\frac{\lambda_m}{\sqrt{\kappa_{ij}}}x\right) + B_{ij,m}\cos\left(\frac{\lambda_m}{\sqrt{\kappa_{ij}}}x\right) \quad (20)$$

Therefore, the general solution to problem (11) is the linear combination of the $\Gamma(t) \cdot \psi_{ij,m}(x)$, which is shown by equation (21).

$$\hat{\sigma}_{ij}(x,t) = \sum_{m=1}^{\infty} C_m e^{-\lambda_m^2 t}\psi_{ij,m}(x) \quad (21)$$

where the eigenvalues λ_m and coefficients $A_{ij,m}$, $B_{ij,m}$,C_m are to be determined by boundary conditions and initial conditions. Finally the original transient hydrostatic stress $\sigma(x,t)$ is obtained as $\sigma(x,t) = \sigma(x,\infty) - \hat{\sigma}(x,t)$.

C. Eigenvalues and Eigenfunctions

The eigenvalues λ_m and eigenfunctions $\psi_{ij,m}(x)$ are essential for the accurate solution. Specifically, eigenvalues λ_m are of the top priority because they are the key parameters in both the transient part $\Gamma(t)$ and eigenfunctions $\psi_{ij,m}(x)$ for the solution. However, it's not trivial to determine the eigenvalues for general interconnect trees, in contrast to the simple case of multi-segment wires described in [12]. As a matter of fact, the eigenvalues for interconnect trees could only be determined numerically by searching for those eigenvalues satisfying the general solution (20) and boundary conditions (12) (13).

The basic idea is to substitute general solutions (20) to boundary conditions (12) (13) and find the eigenvalues λ_m which result in non-trivial solution of eigenfunctions. Utilizing the fact the eigenfunctions are continuous on boundaries of branch (12), we assume the eigenfunctions values on the both ends of the branch ij as $\psi_{i,m}$ and $\psi_{j,m}$. Given those values, the eigenfunction on branch ij is immediately determined by solving following equations (22)

$$\begin{aligned}\psi_{i,m} &= A_{ij,m}\sin(\omega_{ij,m}x_i) + B_{ij,m}\cos(\omega_{ij,m}x_i)\\ \psi_{j,m} &= A_{ij,m}\sin(\omega_{ij,m}x_j) + B_{ij,m}\cos(\omega_{ij,m}x_j)\end{aligned} \quad (22)$$

where $\omega_{ij,m}$ is short notation for $\omega_{ij,m} = \frac{\lambda_m}{\sqrt{\kappa_{ij}}}$.

Based on these eigenfunctions, the derivatives on both ends of branch ij could be calculated as following equation.

$$\begin{bmatrix} \nabla\psi_{ij,m}(x_i) \\ \nabla\psi_{ij,m}(x_j) \end{bmatrix} = \begin{bmatrix} -\psi'_{ij,m}(x_i) \\ \psi'_{ij,m}(x_j) \end{bmatrix} = \begin{bmatrix} \omega_{ij,m}\cot(\omega_{ij,m}l_{ij}) & -\omega_{ij,m}\csc(\omega_{ij,m}l_{ij}) \\ -\omega_{ij,m}\csc(\omega_{ij,m}l_{ij}) & \omega_{ij,m}\cot(\omega_{ij,m}l_{ij}) \end{bmatrix} \cdot \begin{bmatrix} \psi_{i,m} \\ \psi_{j,m} \end{bmatrix} \tag{23}$$

The equation (23) are called "edge equations", where $\nabla\psi_{ij,m}(x_i)$ and $\nabla\psi_{ij,m}(x_j)$ are the inward gradients on branch ends x_i and x_j, respectively.

Substituting the edge equations (23) to the BCs (12) (13), the boundary conditions then lead to constraints of the eigenfunction values on ends of branches, which are represented by equation (24).

$$K(\lambda_m)\cdot\psi^* = 0 \tag{24}$$

where matrix $K(\lambda_m)$ consists of combinations of coefficients of edge equations, which depend on eigenvalues λ_m, and $\psi^* = [\psi_{1,m}, \psi_{2,m}, \cdots, \psi_{n,m}]^T$ is the vector of eigenfunction values on nodes of interconnect tree.

There are non-trivial solutions of eigenfunction that satisfy the boundary conditions only if the determinant of K matrix is 0, i.e. $\det(K(\lambda_m)) = 0$ because any K matrix with $\det(K(\lambda_m)) \neq 0$ implies $\psi^* = 0$, which results in a trivial solution of eigenfunction $\psi_{ij,m}(x) = 0$ for all branch ij. Therefore, those λ_m for which $\det(K(\lambda_m)) = 0$ are the eigenvalues that result in non-trivial solution of eigenfunction. As a result, the eigenvalues are determined by solving the equation (25).

$$\det(K(\lambda_m)) = 0 \tag{25}$$

Unfortunately, equation (25) is a complex transcendental equation, which is hard to solve. In order to overcome this difficulty, the Wittrick-Williams algorithm [19] is utilized. The Wittrick-Williams algorithm is based on the equation (26)

$$N(\mu) = \sum_{ij} N_0(\mu) + s\left(K^{\Delta}(\mu)\right) \tag{26}$$

where $N(\mu)$ is the number of eigenvalues not exceeding μ, $N_0(\mu)$ is the number of eigenvalues of decoupled branch not exceeding μ, $K^{\Delta}(\mu)$ is the upper triangluar matrix of $K(\mu)$ matrix using Guassian elimination and $s\left(K^{\Delta}(\mu)\right)$ is the number of negative leading diagonal elements of $K^{\Delta}(\mu)$. Here $N_0(\mu)$ is calculated as the branches are all decoupled by setting Dirichlet BCs on both ends of branch. Based on the $N(\mu)$ calculated for any given interval $[0, \mu]$, the eigenvalues could easily be confined within intervals by bisection. When the intervals containing eigenvalues approach to punctuations, the eigenvalues are localized and determined.

After the eigenvalues λ_m are determined, the linear equations (24) are solved for eigenfunctions. Because $\det(K(\lambda_m)) = 0$, the eigenfunction values ψ^* could only be uniquely determined with respect to some given element $\psi_{i,m}$. In the numerical computation, we prescribe some element to 1 and then the ψ^* is solved by LU solver. Once the ψ^* is solved, the equations (22) give the results of eigenfunctions.

D. Coefficients of Basic Solution to Satisfy Initial Conditions

Once the eigenvalues λ_m and eigenfunctions $\psi_{ij,m}(x)$ are determined, the solution (21) as a linear combination of basic solutions $\Gamma(t)\cdot\psi_{ij,m}(x)$ are to be specified in terms of the coefficients of the linear combination C_m. The coefficients C_m would be solved by set the solution (21) to satisfy the initial conditions, as shown by equation (27).

$$\hat{\sigma}_0(x) = \hat{\sigma}(x, t=0) = \sum_{m=1}^{\infty} C_m\psi_{ij,m}(x) \tag{27}$$

Since the eigenfunctions are orthogonal to each other, which means inner product of eigenfunctions $\langle\psi_{m_1}(x)\cdot\psi_{m_2}(x)\rangle = \sum_{ij} w_{ij}\int_{x_i}^{x_j}\psi_{ij,m_1}(x)\cdot\psi_{ij,m_2}(x)dx = 0$ for eigenvalues $\lambda_{m_1} \neq \lambda_{m_2}$, the coefficients C_m could be obtained by calculating the inner product of each eigenfunctions $\psi_m(x)$ to the initial conditions $\hat{\sigma}_0(x)$, as shown by equation (28).

$$C_m = \frac{\langle\psi_m(x)\cdot\hat{\sigma}_0(x)\rangle}{\langle\psi_m(x)\cdot\psi_m(x)\rangle} = \frac{\sum_{ij} w_{ij}\int_{x_i}^{x_j}\psi_{ij,m}(x)\cdot\hat{\sigma}_0(x)dx}{\sum_{ij} w_{ij}\int_{x_i}^{x_j}\psi^2_{ij,m}(x)dx} \tag{28}$$

Here the norm of eigenfunctions $\langle\psi_m(x)\cdot\psi_m(x)\rangle$ could be calculated analytically as the following equation (29).

$$\begin{aligned}\langle\psi_m(x)\cdot\psi_m(x)\rangle &= \sum_{ij} w_{ij}\int_{x_i}^{x_j}\psi^2_{ij,m}(x)dx = \sum_{ij} w_{ij} \\ &\cdot\left(\frac{(\psi^{*2}_{i,m}+\psi^{*2}_{j,m})}{\sin^2(\omega_{ij,m}l_{ij})\,\omega_{ij,m}}\left[\frac{\omega_{ij,m}l_{ij} - \sin(\omega_{ij,m}l_{ij})\cos(\omega_{ij,m}l_{ij})}{2}\right]\right. \\ &\left.+\frac{\psi^*_{i,m}\psi^*_{j,m}}{\sin^2(\omega_{ij,m}l_{ij})\,\omega_{ij,m}}\left[\sin(\omega_{ij,m}l_{ij}) - \omega_{ij,m}l_{ij}\cos(\omega_{ij,m}l_{ij})\right]\right)\end{aligned} \tag{29}$$

Generally the inner product of eigenfunctions and initial stress distribution $\langle\psi_m(x)\cdot\hat{\sigma}_0(x)\rangle$ could be calculated numerically by fast fourier transform [20]. However, if a stress distribution $f(x)$ on the interconnect tree is a piece-wise-linear (PWL) function that satisfies the boundary conditions, then its inner product to eigenfunctions could be computed as equation (30). The proof is skipped due to the lack of space. Notice that the initial stress distribution $\hat{\sigma}_0(x) = \sigma(x,\infty) - \sigma_T$ happens to be such a PWL function. Therefore, the inner product of eigenfunctions and initial stress distribution could also be calculated analytically.

$$\begin{aligned}\langle\psi_m(x)\cdot f(x)\rangle = \sum_{ij} -\frac{w_{ij}}{\omega^2_{ij,m}l_{ij}}&\left([f_{ij}(x_j) - f_{ij}(x_i)]\right. \\ &\left.\cdot[\psi_{ij,m}(x_i) - \psi_{ij,m}(x_j)]\right)\end{aligned} \tag{30}$$

IV. Transient Analysis of Hydrostatic Stress Evolution in Void Growth Phase

The same technique that used in void nucleation phase could be applied to transform the IBVP problem in void growth phase to homogeneous problem. This could be verified by

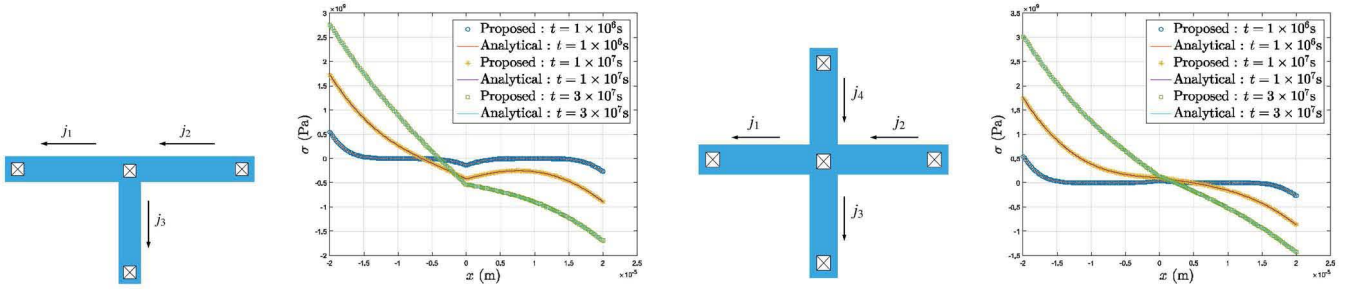

Fig. 3. The T-shape interconnect tree with branch length $2\times10^{-5}m$ and current densities $j_1 = 4\times10^{10}A/m^2$,$j_2 = 2\times10^{10}A/m^2$,$j_3 = 1\times10^{10}A/m^2$ (a) and hydrostatic stress evolution on it (b). The cross-shape interconnect tree with branch length $2 \times 10^{-5}m$ and current density $j_1 = 4 \times 10^{10}A/m^2$,$j_2 = 2 \times 10^{10}A/m^2$,$j_3 = -2 \times 10^{10}A/m^2$,$j_4 = 1 \times 10^{10}A/m^2$, (c) and hydrostatic stress evolution on it (d).

checking the boundary condition (6) still being homogeneous after transformation $\hat{\sigma}(x,t) = \sigma(x,\infty) - \sigma(x,t)$. Notice that the steady state stress $\sigma(x,\infty)$ here has been changed to satisfy the BC (6). Using the zero-flux equation (8) for steady state stress as well as BC (6) , $\sigma(x_\ell,\infty)$ could be readily decided. As a consequence, $\sigma(x,\infty)$ in void growth phase will then be calculated with the help of equation (9). Since the steady state stress $\sigma(x,\infty)$ and transient stress $\sigma(x,t)$ both satisfy the BC (6), the transformed stress $\hat{\sigma}(x,t)$ will satisfy the BC (31).

$$\left.\frac{\partial\hat{\sigma}(x,t)}{\partial x}\right|_{x=x_\ell} = \frac{\hat{\sigma}(x_\ell,t)}{\delta} \tag{31}$$

The difference of calculation of transient hydrostatic stress between void growth phase and void nucleation phase is that the new boundary condition (31) has to be taken into consideration when building the K matrix for determination of eigenvalues and eigenfunctions. To satisfy the BC (31), the following equation (32) is used when building the K matrix.

$$\omega_{\ell j,m}\csc(\omega_{\ell j,m}l_{\ell j})\psi_{j,m} - \omega_{\ell j,m}\cot(\omega_{\ell j,m}l_{\ell j})\psi_{\ell,m} = \psi_{\ell,m}/\delta \tag{32}$$

where ℓj is a branch with one end ℓ at void nucleation.

The rest of steps to solve for the transient stress $\sigma(x,t)$ in void growth phase are the same as those in void nucleation phase, described in previous section III.

V. Experimental Results and Discussions

A. Accuracy of the Eigenfunction-based Transient Hydrostatic Stress Analysis Method

In order to validate the accuracy of the proposed method, the experimental results of transient hydrostatic stress evolution in void nucleation phase are compared with the analytical solutions in [11]. Since only typical interconnect structures, including 3 terminals, 4 terminals and 5 terminals junctions, are analyzed in [11], we compare the transient solutions of the proposed method to those from [11] for these wire structures. Figure 3 shows the structures of interconnect, current density and the transient hydrostatic stress evolution in the void nucleation phase. Since [11] has not provide the analytical solution for the stress evolution in void growth phase, we compare

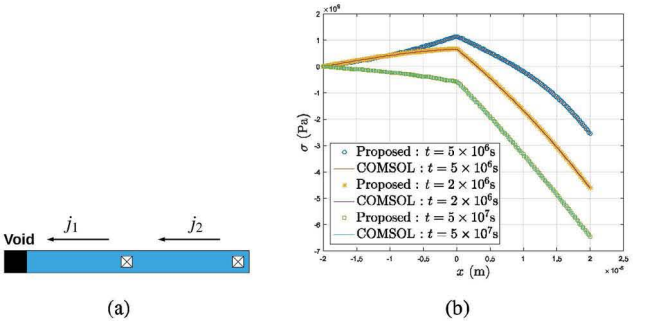

Fig. 4. The 3 terminal interconnect tree with branch length $2 \times 10^{-5}m$ and current densities $j_1 = 2 \times 10^{10}A/m^2$,$j_2 = 6 \times 10^{10}A/m^2$ (a) and hydrostatic stress evolution on it in void growth phase (b).

solutions of our method to the results of the recognized FEA tool COMSOL. Figure 4 shows the results of stress evolution of a 3-terminal interconnect tree in the void growth phase.

In both cases, the proposed method is accurate enough comparing to the results of analytical solution or COMSOL simulation, with max error 0.2%. As a matter of fact, the accuracy of proposed method depends on the number of eigenfunctions used to represent the transient solution. The more eigenfunctions used, the more accurate the solution is. The sufficient number of eigenfunctions depends on the spatial variance of current density. For experiments here,the number of eigenfunctions is chosen to be a typical value of 200.

Notice that our method could compute transient stress evolution for arbitrarily complex interconnect trees beyond these typical structures , which will be demonstrated in next section V-B.

B. Efficiency of the Eigenfunction-based Transient Hydrostatic Stress Analysis Method

In order to demonstrate the efficiency of our method, a multi-branch interconnect tree of n consecutive T-junctions is proposed as the testcase for performance, as shown by Figure 5. Notice that there are $2n+1$ branches on the testing interconnect trees. We then compare the performance of the

proposed method and FDM [10] with increasing number of n to show the efficiency. Both methods solve the transient hydrostatic solution for time $t = 2 \times 10^7 s$. The proposed method is set to analyze the transient solution with the number of eigenfunctions being a typical value 200, which ensures sufficient accuracy. For the FDM, the interconnect trees are discretized to 10 grid per branch spatially and time step $\Delta t = 2 \times 10^5 s$ to run the simulation. For the sake of performance comparision, our method is also set to solve for the stress distribution on the 10 grid points on each branch, which is not necessary in practical EM analysis where only stresses on junction nodes are of interests.

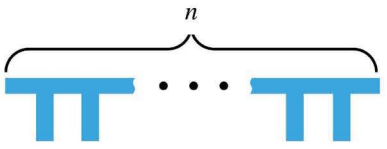

Fig. 5. n T-junctions interconnect structure.

In addtion, we also tested the time costs of the 3 major steps of the proposed method : 1. Calculate the eigenvalues and eigenfunctions with given boundary conditions. 2. Calculate the coefficients of eigenfunctions with given current density and initial stress distribution. 3. Compute the transient hydrostatic solution distribution at time t using the eigenfunctions. In the simulation, the eigenvalues and eigenfunctions need be calculated only once no matter how many transient hydrostatic stresses to solve. Moreover, as long as the current density distribution remains the same, it is not necessary to calculate the coefficients of eigenfunctions again. As a result, the only repetitive computational cost left is that of computing the transient hydrostatic stress as the linear combination of eigenfunctions, which is significantly cheaper.

The proposed method is implemented in C++ and tested on a linux workstation with a 3.6GHz dual-core CPU and 8GB memory. The FDM [10] is tested on a linux server with 2×16 core 3.3GHz CPU and 128GB memory. Table I shows the time costs of the proposed method and FDM for varying n T-junctions. Here t_{fdm} is the time cost of FDM according to above metioned discretization schema. t_{eig}, t_{coef}, t_σ are the time costs of the 3 steps of the propposed method, namely eigenvalues and eigenfunctions calculation, coefficients calculation and transient stress calculation, respectively. In addtion to the time cost t_{total} of direct calculation of stress at $t = 2 \times 10^7 s$, we also present the time cost t_{all} of calculating the transient stresses for all time steps $\Delta t, 2\Delta t, 3\Delta t, \cdots, 100\Delta t$. Notice that calculating for all time steps is also for the sake of comparision to FDM. In contrast to FDM, our method could just skip the time points at which the hydrostatic stress is irrelevant to EM failure in practical EM analysis. See next section for more discussion on this. As we can see from Table I, the proposed method is 10X$\sim$100X times faster than FDM. Moreover, the proposed method scales better than FDM for larger interconnect trees. The FDM fails to solve the stress for huge n larger than 10000. Figure 6 shows the time costs of the 3 parts of the proposed method for varying n T-junctions. As we can see, calculation of eigenvalues and eigenfunction costs the most, while it runs only once. The repetitive work of step 3 costs least. All the computational costs of 3 steps increase linearly with the size of interconnect tree, which means the proposed method scales well for the large interconnect trees.

TABLE I
RUNTIME COMPARASION OF THE PROPOSED METHOD AND FDM.

n	The Proposed Method (sec)					FDM(sec)
	t_{eig}	t_{coef}	t_σ	t_{total}	t_{all}	t_{fdm}
20	0.099	0.016	0.0076	0.123	0.63	0.32
50	0.152	0.026	0.0094	0.187	1.30	1.61
100	0.485	0.062	0.0180	0.566	2.89	7.20
200	0.960	0.137	0.0358	1.133	5.21	44.5
500	2.372	0.407	0.1356	2.915	14.6	298.4
700	2.406	0.692	0.1632	3.262	17.8	611.5
900	3.171	0.919	0.1926	4.283	23.8	1114.5
1000	5.423	0.832	0.1723	6.428	25.8	1443.9
1200	4.340	1.822	0.2757	6.439	36.8	2080.4
1500	5.856	1.837	0.3442	8.123	44.1	3525.4
1700	6.713	2.242	0.3516	9.307	48.5	5581.6
1900	6.981	2.346	0.3489	9.676	50.3	8053.1
2000	10.53	2.056	0.3579	12.95	51.4	15651.2
10000	49.71	13.83	2.5851	66.13	236.7	NA
50000	231.2	56.86	11.024	299.1	1393.6	NA
100000	441.8	141.7	26.984	610.5	2969.9	NA

C. Discussion

Since the proposed method avoids discretization either spatially or temporally, it can skip the calculation of hydrostatic stress on any location or at any time if this stress is irrelevant to the EM failure. In contrast, the FDM has to calculate all stress distribution at all time steps because the discretized hydrostatic stresses on the interconnect tree are coupled together. For example, the effective algorithms proposed in [6] to find out the void nucleation time t_{nuc}, such as Newton's method or bisection method, could still be utilized with our method, but more accurate since transient hydrostatic stress is provided instead of steady-state stress. Moreover, the proposed method provides the analytical solution of the hydrostatic stress, although eigenvalues and eigenfunctions have to be determined numerically.The proposed method becomes naturally to the analytical solutions for single wire [9] or 1D multi-segment wires [12], given these specific interconnect structures. Therefore, the proposed method shares the same characteristics and advantages as those of the analytical solutions.

VI. CONCLUSION

In this paper, we have proposed an accurate transient analysis method for the hydrostatic stress evolution for multi-branch interconnect trees to facilitate fast electromigration assessment. The proposed method, which is based on eigenfunctions technique, solves the 2-dimentional Korhonen's equation for multi-branch interconnect trees stressed with different current

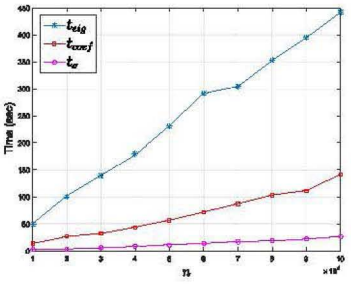

Fig. 6. Time costs of 3 steps of the proposed method with varing n.

densities and non-uniformly distributed thermal effects. The proposed method can also accommodate the pre-existing residual stresses coming from thermal or other stress sources. The new method overcomes the difficulties of previous methods by improving the accuracy and efficiency. The transient hydrostatic stress evolution could be calculated accurately by the proposed method so that the void nucleation and void growth could be simulated precisely. Our numerical results show that the proposed method is 10X∼100X times faster than finite difference method and scales better for larger interconnect trees. Because of the benefits of the proposed method, the EM verification based on our method could be carried out accurately without sacrificing the efficiency for large scale on-chip interconnect networks.

REFERENCES

[1] J. Black, "Electromigration - a brief survey and some recent results," *IEEE Transactions on Electron Devices*, vol. 16, no. 4, pp. 338–347, Apr. 1969.

[2] I. A. Blech, "Electromigration in thin aluminum films on titanium nitride," *Journal of Applied Physics*, vol. 47, no. 4, pp. 1203–1208, Apr. 1976.

[3] S. Chatterjee, V. Sukharev, and F. N. Najm, "Fast physics-based electromigration checking for on-die power grids," in *Proceedings of the 35th International Conference on Computer-Aided Design - ICCAD '16*, New York, New York, USA: ACM Press, 2016, pp. 1–8.

[4] M. Hauschildt, C. Hennesthal, G. Talut, O. Aubel, M. Gall, K. B. Yeap, and E. Zschech, "Electromigration early failure void nucleation and growth phenomena in cu and cu(mn) interconnects," in *2013 IEEE International Reliability Physics Symposium (IRPS)*, IEEE, Apr. 2013, pp. 2C.1.1–2C.1.6.

[5] J. Lloyd, "New models for interconnect failure in advanced ic technology," in *2008 15th International Symposium on the Physical and Failure Analysis of Integrated Circuits*, IEEE, Jul. 2008, pp. 1–7.

[6] X. Huang, A. Kteyan, X. Tan, and V. Sukharev, "Physics-based electromigration models and full-chip assessment for power grid networks," *IEEE Transactions on Computer-Aided Design of Integrated Circuits and Systems*, vol. PP, no. 99, pp. 1–1, 2016.

[7] M. Pathak, J. Pak, D. Z. Pan, and S. K. Lim, "Electromigration modeling and full-chip reliability analysis for beol interconnect in tsv-based 3d ics," in *2011 IEEE/ACM International Conference on Computer-Aided Design (ICCAD)*, IEEE, Nov. 2011, pp. 555–562.

[8] V. Sukharev, X. Huang, H.-B. Chen, and S. X.-D. Tan, "Ir-drop based electromigration assessment: parametric failure chip-scale analysis," in *2014 IEEE/ACM International Conference on Computer-Aided Design (ICCAD)*, IEEE, Nov. 2014, pp. 428–433.

[9] M. A. Korhonen, P. Borgesen, K. N. Tu, and C.-Y. Li, "Stress evolution due to electromigration in confined metal lines," *Journal of Applied Physics*, vol. 73, no. 8, p. 3790, Apr. 1993.

[10] C. Cook, Z. Sun, T. Kim, and S. X. D. Tan, "Finite difference method for electromigration analysis of multi-branch interconnects," in *2016 13th International Conference on Synthesis, Modeling, Analysis and Simulation Methods and Applications to Circuit Design, SMACD 2016*, 2016, pp. 1–4.

[11] H.-b. Chen, S. X. Tan, S. Member, X. Huang, T. Kim, and V. Sukharev, "Analytical modeling and characterization of electromigration effects for multi-branch interconnect trees," *IEEE Transactions on Computer-Aided Design of Integrated Circuits and Systems*, vol. PP, no. 99, pp. 1–16, 2016.

[12] X. Wang, H. Wang, J. He, S. X.-D. Tan, Y. Cai, and S. Yang, "Physical-based electromigration modeling and assessment for multi-segment interconnects in power grid networks," in *2017 Design, Automation and Test in Europe Conference*, 2017, pp. 1727–1732.

[13] J. J. Clement, "Reliability analysis for encapsulated interconnect lines under dc and pulsed dc current using a continuum electromigration transport model," *Journal of Applied Physics*, vol. 82, no. 12, p. 5991, 1997.

[14] M. E. Sarychev, Y. V. Zhitnikov, L. Borucki, C.-L. Liu, and T. M. Makhviladze, "General model for mechanical stress evolution during electromigration," *Journal of Applied Physics*, vol. 86, no. 6, p. 3068, 1999.

[15] V. Sukharev, A. Kteyan, E. Zschech, and W. Nix, "Microstructure effect on em-induced degradations in dual inlaid copper interconnects," *IEEE Transactions on Device and Materials Reliability*, vol. 9, no. 1, pp. 87–97, Mar. 2009.

[16] V. Sukharev, A. Kteyan, and X. Huang, "Postvoiding stress evolution in confined metal lines," *IEEE Transactions on Device and Materials Reliability*, vol. 16, no. 1, pp. 50–60, Mar. 2016.

[17] X. Huang, T. Yu, V. Sukharev, and S. X.-D. Tan, "Physics-based electromigration assessment for power grid networks," in *Proceedings of the The 51st Annual Design Automation Conference on Design Automation Conference - DAC '14*, 2014, pp. 1–6.

[18] Z. Sun, E. Demircan, M. D. Shroff, T. Kim, X. Huang, and S. X. D. Tan, "Voltage-based electromigration immortality check for general multi-branch interconnects," in *2016 IEEE/ACM International Conference on Computer-Aided Design (ICCAD)*, Nov. 2016, pp. 1–7.

[19] W. H. Wittrick and F. W. Williams, "A general algorithm for computing natural frequencies of elastic structures," *The Quarterly Journal of Mechanics and Applied Mathematics*, vol. 24, no. 3, pp. 263–284, 1971.

[20] William H. Press, S. A. Teukolsky, W. T. Vetterling, and B. P. Flannery, *Numerical Recipes*. Cambridge University Press, 2007.